Chemical Engineering Journal 160 (2010) 176–184

Contents lists available at ScienceDirect

Chemical Engineering Journal

journal homepage: www.elsevier.com/locate/cej

Comparative evaluation of polymer surface functionalization techniques before iron oxide deposition. Activity of the iron oxide-coated polymer films in the photo-assisted degradation of organic pollutants and inactivation of bacteria

F. Mazille[b], A. Moncayo-Lasso[a], D. Spuhler[b], A. Serra[c], J. Peral[c], N.L. Benítez[a], C. Pulgarin[b,*]

[a] Group of Advanced Oxidation Processes (GAOX), Department of Chemistry, Universidad del Valle, Cali, Colombia
[b] Institute of Chemical Sciences and Engineering, SB, GGEC, Ecole Polytechnique Fédérale de Lausanne, 1015 Lausanne, Switzerland
[c] Departament de Quimica, Edifici Cn, Universitat Autonoma de Barcelona, E-08193 Bellaterra, Barcelona, Spain

ARTICLE INFO

Article history:
Received 5 January 2010
Received in revised form 15 March 2010
Accepted 16 March 2010

Keywords:
Polymer surface modification
Photo-Fenton
SODIS
Bacterial inactivation
Photocatalytic functionalization

ABSTRACT

The preparation of iron oxide-coated polymer films and their photocatalytic activity in organic pollutants degradation and bacterial inactivation is described. Polyvinyl fluoride (PVF), polyethylene (PE) and polyethylene terephtalate (PET) films were used as catalyst supports. Polymer surfaces were functionalized by vacuum-UV radiation (V-UV) and radio-frequency plasma (RF-P); and also by photo-Fenton oxidation (P-FO) and TiO_2 photocatalysis (Ti-PC) in solution. These pre-treatments were performed to improve iron oxide adhesion on the commercial polymer surface. The functionalized polymers films (P^f) were afterward immersed in an aqueous solution for the deposition of iron oxide layer by hydrolysis of $FeCl_3$. The photocatalytic activities of iron oxide-coated functionalized polymers films (P^f-Fe oxide) prepared by different methods were compared during hydroquinone degradation in presence of H_2O_2. RF-P and Ti-PC pre-treated polymers showed significantly higher photocatalytic activity and long-term stability during processes leading to pollutant abatement, if compared with not treated ones (NT), although similar leaching of iron was observed for all the materials. PET bottles (PET_b) were used as reactor and catalyst supports. The produced $PET_b{}^f$-Fe oxide surfaces were efficient in photo-assisted bacterial inactivation in the presence of H_2O_2, and no dissolved iron species were detected in solution.

1. Introduction

The photo-assisted Fenton oxidation is a promising alternative to obtain drinking water from contaminated water since it leads to water remediation under solar light irradiation. Homogeneous photo-Fenton process (Fe^{2+}/H_2O_2/light) is a method for the treatment of water containing bio-recalcitrant organic pollutants [1] that has also shown to be effective in bacterial disinfection [2–5]. However, this process has some disadvantages such as the need of a narrow operational pH range (pH 3–5) and sludge formation. Therefore, an end of pipe treatment is needed to neutralize pH and to recover catalyst since the maximum dissolved iron concentration allowed in the European Union legislation for drinking water is 0.2 mg/L [6]. To overcome these limitations the use of dispersed iron oxides particles such as hematite, goethite or akaganeite as solid photo-Fenton catalyst has been proposed [7]. The immobilization of iron oxides on supports and the evaluation of their photocatalytic activity have shown growing interest during the present decade [8–14].

Solar water disinfection (SODIS) is a low cost method for treating microbial contaminated drinking water in transparent plastic bottles [15]. Nevertheless this method presents some disadvantages such as temperature dependency and re-growth of microorganism. The application of photo-Fenton could solve the SODIS limitations and lead to the simultaneous disinfection and degradation of xenobiotics and natural organic matter.

The use of polymer film or bottles as supports for iron oxides deposition was chosen for this study although it induces several drawbacks that have to be overtaken: (i) commercial polymer films surfaces are slick, limiting iron oxide crystal nucleation and its adhesion to the substrate; (ii) since the point of zero charge of iron oxide is around pH 8 [16] their surface is positively charged at neutral and acidic pHs. Thus, the presence of electron donor groups as carboxylic acids on polymer support surface is required to bind strongly iron oxide particles; and (iii) polymer films are destroyed under high temperature and are slowly degraded under solar irradiation. Although commercial available polymers have surface roughness, electron donor groups, relatively high melting point and high stability under solar light, many commonly used

* Corresponding author. Tel.: +41 21 693 47 20; fax: +41 21 693 61 61.
E-mail address: cesar.pulgarin@epfl.ch (C. Pulgarin).

1385-8947/$ – see front matter © 2010 Elsevier B.V. All rights reserved.
doi:10.1016/j.cej.2010.03.035

and low cost polymers films such as polyethylene (PE), polyethylene terephtalate (PET), etc., do not show such properties. Since those polymer films are widely used in packaging or bottles, they can be recycled as photocatalyst supports, but a functionalization of their surface is required.

Radio frequency plasma (RF-P) and vacuum ultraviolet (V-UV) treatment have been applied for polymer surface functionalization [17]. RF-P and V-UV treatments were applied to textiles to promote the deposition of silver [18] or TiO_2 [19] for antibacterial applications.

Photocatalytic treatments such as TiO_2 photocatalysis (Ti-PC) and photo-Fenton oxidation (P-FO) are attractive alternatives for polymer surface modification because of the mild conditions needed (solar light, low temperature and atmospheric pressure). Besides, Ti-PC treatment of polymer films was studied recently for increasing adhesion strength before electroless Cu plating [20] and iron oxide deposition [21].

This investigation is directed toward the fixation and photocatalytic performance of iron oxide on different polymer films previously functionalized by different methods. To compare the photo-activity as a function of preparation procedure (different functionalization methods) hydroquinone was selected as a model compound. The ability of these photocatalysts to inactivate bacteria was studied using *Eschecheria coli* as a model microorganism.

2. Experimental

2.1. Chemicals

Hydroquinone, NaOH, HNO_3, $FeCl_3{\cdot}6H_2O$, $FeSO_4$, ferrizine, hydroxylamine hydrochloride, acetate buffer (pH 4.65) were Fluka p.a. reagents (Buchs, Switzerland) and used as received. Hydrogen peroxide (35%, w/w) was supplied by Merck AG (Darmstadt, Germany). TiO_2 P25 (anastase to rutile weight ratio between 70:30 and 80:20) was supplied by Degussa. The polyvinyl fluoride (PVF), polyethylene (PE) and polyethylene terephtalate (PET) films were 72 μm thick and were supplied by Goodfellow (Cambridge Ltd., United Kingdom). The PET bottles (polypropylene cover, 100 mL, diameter: 4.8 cm, heigth: 9.5 cm) were supplied by Reactolab SA (Servion, Switzerland). Solutions were prepared with Millipore water (18.2 MΩ cm at 25 °C).

2.2. Photo-reactor and irradiation procedures

The photo-reactor setup for organic pollutants degradation and the lamp characteristics have been reported elsewhere [21]. Briefly, the irradiation experiments were started at room temperature (20 °C), but during degradation process the temperature reached 30 °C. Control experiments in the dark were performed in similar conditions. Three Pyrex glass reactors containing an internal PVC cylinder as photocatalyst film support were placed in parallel inside the solar box. The degradation experiments for the hydroquinone (HQ) solutions (0.18 mM) and H_2O_2 1.6 mM were performed under recirculation.

For bacterial inactivation, experiments were carried out in batch mode in a 100 mL Pyrex glass reactor (4 cm diameter, 9 cm height, and 100 mL volume, lab made reactor, Verrerie du Jorat, Corcelles-le-Jorat, Switzerland) or PET bottles reactors placed in parallel inside the solar box. The polymer photocatalyst films ($PET^{Ti\text{-}PC}$-Fe oxide 9 cm × 12.5 cm) were placed around the internal surface of the Pyrex photoreactor without internal support. PET bottles were used both as reactor and photocatalyst substrate. The temperatures during the experiments were always below 38 °C then thermal inactivation of microorganisms can be excluded.

2.3. Analysis of the irradiated solutions

The quantitative determination of organic compounds was carried out by HPLC chromatography using a LC system HPLC-UV: Shimatzu LC-2010A equipped with a UV detector. Samples, injected via autosampler, were eluted at a flow rate of 1 mL/min through a column (nucleosil C18 Marcherey Nagel) and using a 60:40 acetonitrile: 1% (v/v) aqueous acetic acid solution as mobile phase. Total organic carbon (TOC) was monitored via a Shimadzu 500 instrument equipped with an ASI automatic sample injector. The peroxide concentrations were assessed by Merkoquant® paper at levels between 0.5 and 25 mg/L. The total iron concentration in the irradiated solutions was measured by complexation with Ferrozine® (Aldrich 16.060-1) in the presence of hydroxylamine hydrochloride and an acetate buffer (pH 4.65) [22].

2.4. Bacterial strain and growth media

Bacterial strains. The *E. coli* strain K-12 (MG1655) was used for all the disinfection experiments and supplied by DSMZ (German Collection for Microorganisms and Cell cultures, Darmstadt, Germany). *E. coli* K-12 is a non-pathogenic and close to the wild-type *E. coli*, a typical indicator bacteria for enteric pathogens.

Sample preparation. Strain samples were stored in cryo-vials containing 20% glycerol at −20 °C. Bacterial pre-cultures were prepared for each experimental series by streaking out a loopfull from the strain sample onto Plate Count Agar (PCA) and subsequent incubation of these plates for 24 h at 37 °C (Heraeus Incubator B 5060 EK-CO2, Heraeus Instruments, Hanau, Germany). From the growing colonies, one was re-plated on a separate PCA and incubated again for 24 h at 37 °C.

Luria–Bertani (LB) broth (10 g Bacto™ Trypton, 5 g Yeast extract, 10 g NaCl per liter) was prepared for each experimental series by suspension in MilliQ and heat-sterilization by autoclave (121 °C, 20 min, VST 500A, LS SECFROID, Blanc Labo, Lonay, Switzerland).

To prepare the bacterial pellet for the photo-inactivation experiments, one colony was picked from the pre-cultures and loop-inoculated into a 50 mL sterile PE Eppendorf flask containing 5 mL of LB broth. The flask was then incubated at 37 °C and 180 rpm in a shaker incubator (Minitron AI 71, IN-3 FORS AG, Bottmingen, Switzerland). After 8 h, cells were diluted (1%, v/v) in a 250 mL Erlenmeyer flasks containing 25 mL of pre-warmed LB broth and incubated at 37 °C for 15 h in Heraeus Incubator until stationary physiological phase was reached. Bacterial growth and stationary phase was monitored by the optical density at 600 nm. Cells were harvested during stationary growth phase by centrifugation (15 min at 5000 × *g* (RCF) and 4 °C) in a universal centrifuge (HERMLE Z 323K, Renggli Laboratory Systems, Renens, Switzerland). The bacterial pellet was re-suspended and washed for 10 min in the centrifuge.

Washing was repeated twice and the bacterial pellet was re-suspended to the initial volume. This procedure resulted in a bacterial pellet containing 1.5×10^8 CFU/mL Washing and re-suspension was done in heat sterilized MilliQ water. At the beginning of each experiment the reactors containing the bacterial suspension were placed in the solar simulator in the dark under magnetic stirring for at least 1 h in order to let bacteria adapt to the new matrix and to allow die-off of the most stress sensitive species. After stabilization of the population, H_2O_2 was added before turning on the lamp.

Plating. Colony forming units (CFU) were monitored by pour plating on PCA. At each data point 1 mL of sample was withdrawn. Exceeding H_2O_2 was neutralized with catalase, aliquots were diluted in 10% steps and poor plated on PCA. Plates were incubated for 24 h at 37 °C and CFU were counted manually.

2.5. Catalyst characterization

The UV–vis spectra of different photocatalysts were recorded on a Varian Cary 5 equipped with an integration sphere.

X-ray photoelectron spectroscopy data were collected by Axis Ultra system (Kratos analytical, Manchester, UK) under ultra-high vacuum condition (<10^{-8} Torr), using a monochromatic Al Kα X-ray source (1486.6 eV) at the laboratory of Chemical Metallurgy at EPFL. The source power was maintained at 150 W (10 mA, 15 kV). The emitted photoelectrons were sampled from a square area of 750 μm × 350 μm. The gold (Au $4f_{7/2}$) and copper (Cu $2p_{3/2}$) lines at 84.0 and 932.6 eV respectively, were used for calibration, and the adventitious carbon 1s peak at 284.6 eV was used as an internal standard to compensate for charging effects.

The surface morphology of the catalysts was investigated using a scanning electron microscope (Phillips XL30 SFEG) equipped with X-ray detector.

3. Results and discussion

3.1. Catalyst preparation and characterization

Photoactive iron oxide was deposited on commercial polymer film substrates. Before use, the films were washed in a diethyl ether:ethanol (1:1) mixture and in MilliQ water in order to eliminate surface contaminants. Then polymer films were functionalized by different methods (V-UV, RF-P, Ti-PC, P-FO) describe in the next paragraphs.

3.1.1. Functionalization with RF-plasma

The polymers films were treated in a RF-plasma (RF-P) cavity (Harricks Corp., 13.56 MHz, power 100 W) at a pressure of 1.0 mbar (leading to so called $PVF^{RF\text{-}P}$). The gas used for the plasma generation was air. Plasma can be broadly defined as a gas containing charged and neutral species. The reactions between those gas-phase species and polymer surface species produce functional groups like hydroxyls, ketones and carboxylic acids. Other reactions induced by the plasma are the polymerization, cross-linking and etching [17].

The functionalization process occurs in the topmost layers and increase with longer treatment time, but remains constant with treatment time >30 min [18]. For this reason the latter time has been chosen for RF-P treatment.

A previous report [24] presented a detail electron spectroscopy for chemical analysis (ESCA) study of the effect of oxygen RF-P treatment on PVF surface which was shown to produce C=O, fluorine loss and a slight loss of carbon atoms (by etching). As the effect of RF-P on PVF was studied elsewhere [24], it is not reported on the present work.

3.1.2. Functionalization with V-UV

The polymer film surface was also functionalized by V-UV irradiation (leading to so called $PVF^{V\text{-}UV}$) using the 185 nm (6 W) line from a 25 W (254 + 185 nm) low pressure mercury lamp (Ebra Corp., Tokyo, Japan). The lamp was a synthetic silica tube. The polymer film was attached around the lamp tube. The gas used was air (0.8 mbar) and the treatment time was 30 min (same treatment time as in [18]). Lower energies than in RF-P are attained by V-UV activation, not allowing the formation of charged oxygen species in the gas phase. Only atomic (O) and excited (O^*) oxygen species are formed. Most of the polymers strongly absorb the V-UV leading to the dissociation of various chemical bonds in polymer molecules and to formation of radicals. The recombination of radicals formed by V-UV photolysis leads to the formation of cross-links. The detachment of hydrogen molecules H_2 induced by V-UV photolysis is responsible for the formation of double bonds in polymer matrix. Besides, V-UV treatment may improve surface mechanical properties and change the polymer surface morphology but without significant etching [17]. A detail investigation on the effect of V-UV radiation on PVF films was reported recently [25]. It was found that with short treatment times (i.e. <24 h) the main effect induced by this treatment was a washing of surface contamination a decrease of fluorine surface concentration and an increase of carbon surface concentration. As the effect of V-UV on PVF was studied elsewhere [25], and because this treatment was not effective to improve iron oxide adhesions (see points 3.2 and 3.3) a surface characterization was not performed on the present work.

3.1.3. Functionalization with photo-Fenton oxidation

The polymer films were attached on a cylindrical steal support and immersed in solutions of Fe^{2+} (50 mg/L) containing H_2O_2 (30 mM) at pH 3. The batch reactor was irradiated in a solar simulator CPS Suntest system (ATLAS). The polymer surface undergoes the photo-Fenton functionalization during 2 h under magnetic stirring irradiation (leading to so called $PVF^{P\text{-}FO}$). The species generated in aqueous phase by photo-Fenton oxidation are radicals such as $OH^\bullet$ or $O_2^{\bullet -}$. As photo-Fenton functionalization was not effective to improve iron oxide adhesions (see points 3.2 and 3.3) the surface characterization of P-FO was not performed.

3.1.4. Functionalization with TiO_2 photocatalysis

The polymer films were attached on a cylindrical steal support and immersed in well dispersed solutions of TiO_2 1 g/L (0.2 g/L in sections 3.2 and 3.3) at natural pH. The batch reactor was irradiated in a solar simulator CPS Suntest system (ATLAS). The polymer surface underwent the TiO_2 photocatalytic functionalization under magnetic stirring during 2 h (4 h for section 3.4 and 3.5 irradiation, leading to so called $PVF^{Ti\text{-}PC}$).

The species generated by Ti-PC treatment are radicals such as hydroxyl and super-oxide, as well as holes and electrons. These reactive species can react with polymer surface. A recent XPS study of Ti-PC functionalization of PVF [21] has shown that this treatment generates a variable density of negative groups (such as C=O, COO^{2-}, etc.) and induced fluorine elimination. Besides TiO_2 particles were found to bind to the freshly functionalized polymer surface generating roughness and supplementary photocatalytic activity. Fig. 1 shows the SEM pictures of PVF before and after the Ti-PC functionalization. The non-modified PVF surface, Fig. 1a, is predominantly smooth. After a TiO_2 PC treatment, aggregated TiO_2 particles cover a significant part of the surface exposed to the light irradiation (Fig. 1b).

3.1.5. Iron oxide coating

To immobilize iron oxide, functionalized polymer films (P^f) were immersed in a solution of $FeCl_3$ 5 g/L (2 g/L for section 3.4 and 3.5) and heated under stirring at 80 °C during 1 h (to produce so called P^f-Fe oxide). Optionally, the composite material was heated in an oven at 100 °C for 1 h. The final films showed a brownish iron oxide coat. Fig. 2 shows the XPS spectrum representative of iron oxide on modified PVF films. The Fe (2p) spectrums of as prepared $PVF^{Ti\text{-}PC}$-Fe oxide (trace a), of $PVF^{Ti\text{-}PC}$-Fe oxide and $PVF^{RF\text{-}P}$-Fe oxide samples after use are pretty similar and unambiguously characteristic of Fe^{3+} in an oxide (Fe $2p_{1/2}$, Fe $2p_{3/2}$ and satellite peaks are at a binding energy of 725, 711 and 719 eV, respectively; the satellite peak is a distinct peak [26]) which suggest that no significant changes in the iron oxidation state occurred after use. Akaganeite [27] is probably the oxide present due to the significant presence of chlorine in the oxide (see Table 1). Various reports confirm this hypothesis, as the thermal hydrolysis of $FeCl_3$ solutions leads mainly to the forma-

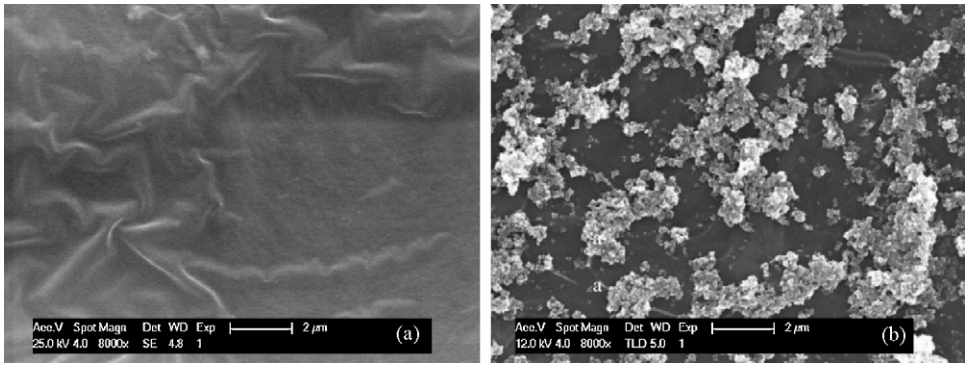

Fig. 1. Scanning electron microscopic images of (a) PVF and (b) $PVF^{Ti\text{-}PC}$.

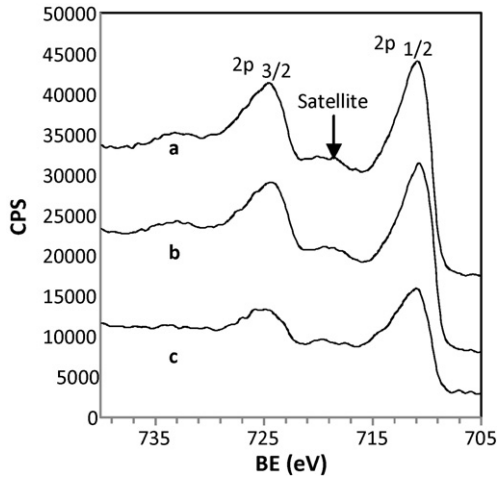

Fig. 2. Fe (2p) core level photoelectron spectrum of (a) as-prepared $PVF^{Ti\text{-}PC}$-Fe oxide and (b and c) $PVF^{Ti\text{-}PC}$-Fe oxide and $PVF^{RF\text{-}P}$-Fe oxide, respectively, after three runs.

Table 1
Atomic composition (atomic percent) of $PVF^{Ti\text{-}PC}$ and $PVF^{Ti\text{-}PC}$-Fe oxide surfaces (results from [21,23]).

Samples	C	O	F	Cl	Ti	Fe
$PVF^{Ti\text{-}PC}$	72.6	16.9	9.3	0	1.3	0
$PVF^{Ti\text{-}PC}$-Fe oxide	35.1	45.1	1.5	1.7	0.3	16.8

tion of akaganeite [28]. Fig. 3 shows the SEM pictures typical of iron oxide-coated polymer surfaces loaded with iron oxide aggregates of about 1 μm. These aggregates are composed of nanoparticles of approximately 50 nm, which seem to cover the polymer surface (Fig. 3b).

3.1.6. Preparation of PET bottles functionalized by Ti-PC and coated with iron oxide

Photoactive TiO_2 and iron oxide were deposited on commercial PET bottles (100 mL) in a similar way than described in the previous sections. Briefly, clean PET bottles were filled up with a 60 mL dispersed suspension of 1 g/L of TiO_2. The bottles were then irradiated in a CPS Suntest system for 2.5 h under magnetic stirring. The functionalized bottles were then emptied, rinsed with miliQ water and filled up with 60 mL of a $FeCl_3$ solution (5 g/L) to carry out forced hydrolysis at 60 °C during 1.5 h. Heating at 95 °C during half an hour in an oven was performed to anneal TiO_2 and iron oxide particles on the PET surface.

3.2. Effect of functionalization on photocatalytic activity of PVF^f-Fe oxide

Fig. 4 shows (i) HQ, (ii) TOC and (iii) dissolved iron concentrations ($[Fe]_d$) over time during degradation experiments mediated by different photocatalysts in the presence of H_2O_2 and light. The pH initially 5.7 decreased to 4.5 after 30 min mostly due to the formation of short acidic degradation intermediates. Fig. 4(i) shows that HQ was resistant to direct photolysis by simulated solar light alone (trace o).

During the degradation of HQ mediated by PVF^{NT}-Fe oxide (trace a Fig. 4(i)), $PVF^{P\text{-}FO}$-Fe oxide and $PVF^{V\text{-}UV}$-Fe oxide (both represented by trace b Fig. 4(i)), the HQ degradation was low during the first 30 min of treatment but was complete at 120 min. The initial phase is slow and then fast degradation sets seems to be due to homogeneous photo-Fenton oxidation, since after 60 min the concentration of dissolved iron ($[Fe]_d$) detected is around 0.3 mg/L (Fig. 4(iii)). For the photo-assisted degradations (Fig. 4(i)) mediated by $PVF^{RF\text{-}P}$-Fe oxide (trace c) and $PVF^{Ti\text{-}PC}$-Fe oxide (trace d), the initial degradation (first 30 min) was important with about 30 and 60% of HQ degradation, respectively.

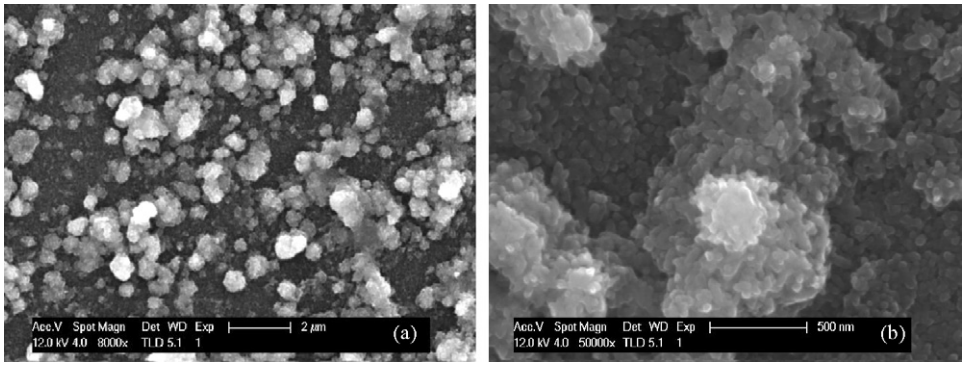

Fig. 3. Scanning electron microscopic images of as prepared $PVF^{Ti\text{-}PC}$-Fe oxide.

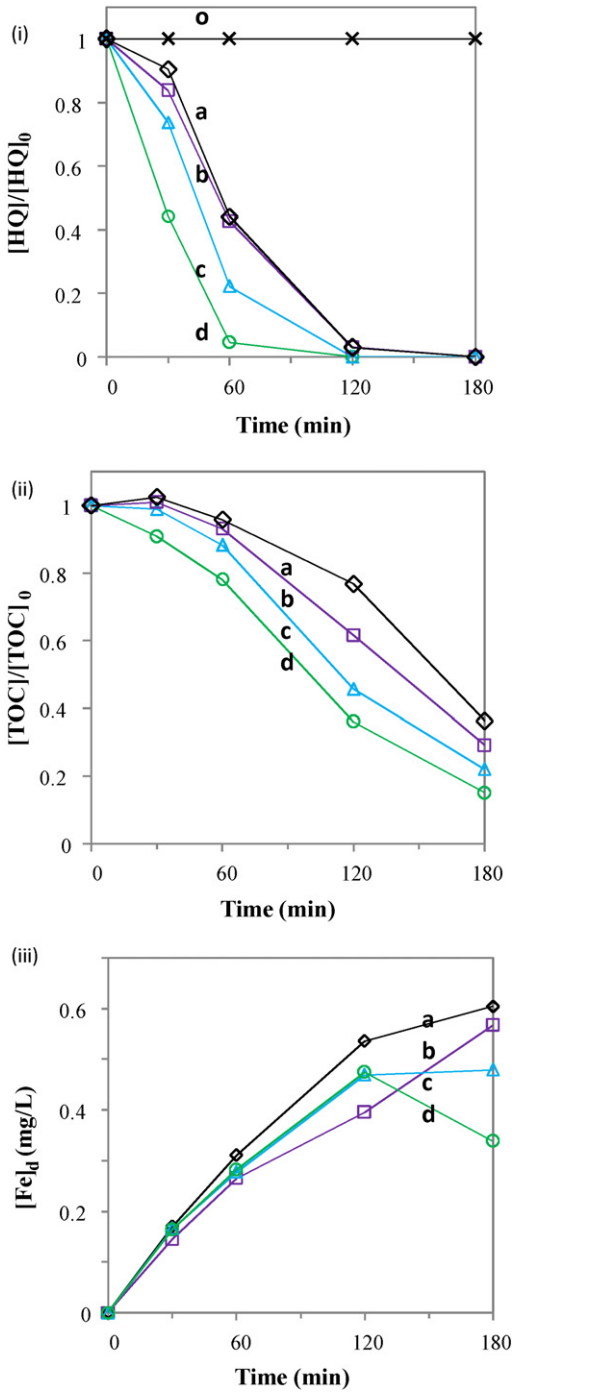

Fig. 4. Reduction of (i) HQ concentration, (ii) TOC and variation of (iii) $[Fe]_d$ during degradation of 0.18 mM of HQ at initial pH 5.7, in presence of 1.6 mM H_2O_2, 75 cm^2 of catalyst under solar simulation (light): (o) photolysis; (a) PVF-Fe-oxide; (b) $PVF^{V\text{-}UV}$-Fe oxide and $PVF^{P\text{-}FO}$-Fe oxide*; (c) $PVF^{RF\text{-}P}$-Fe oxide; (d) $PVF^{Ti\text{-}PC}$-Fe oxide. The traces represent an average over three runs. *Due to similar result obtained for $PVF^{V\text{-}UVC}$-Fe oxide and $PVF^{P\text{-}FO}$-Fe oxide trace (b) represent the results relative to these two catalysts.

Fig. 4(ii) shows that during the first 30 min. of irradiation, the TOC slightly increased for PVF^{NT}-Fe oxide (trace a), $PVF^{V\text{-}UV}$-Fe oxide and $PVF^{P\text{-}FO}$-Fe oxide (both in trace b), due to a degradation of the polymer substrate, but remains constant for $PVF^{RF\text{-}P}$-Fe oxide. After that the TOC begins to decrease and about 25, 40 and 55% of mineralization was observed for PVF-Fe oxide, both $PVF^{V\text{-}UV}$-Fe oxide and $PVF^{P\text{-}FO}$-Fe oxide, and, $PVF^{RF\text{-}P}$-Fe oxide, respectively, after 120 min of treatment. In contrast, a significant TOC decrease

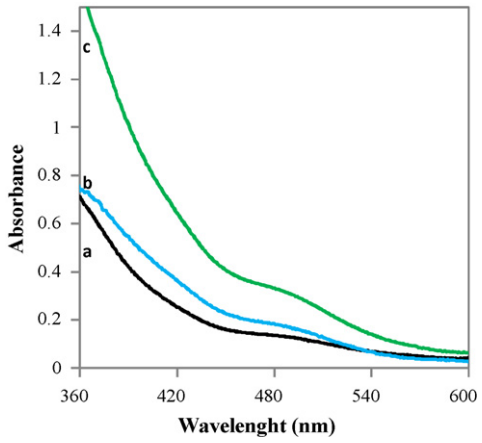

Fig. 5. UV–vis absorption spectrum of (a) PVF-Fe oxide, $PVF^{V\text{-}UV}$-Fe oxide, $PVF^{P\text{-}FO}$-Fe oxide; (b) $PVF^{RF\text{-}P}$-Fe oxide; (c) $PVF^{Ti\text{-}PC}$-Fe oxide.

was observed from the beginning, when $PVF^{Ti\text{-}PC}$-Fe oxide was used and 65% of TOC was mineralized after 120 min of treatment.

Fig. 4(iii) shows that the leaching of iron was similar for the five tested catalysts. Only for the $PVF^{Ti\text{-}PC}$-Fe oxide, the $[Fe]_d$ decreased slightly at the end of the treatment. This fact suggests that dissolved iron species were re-adsorbed on the catalyst surface possibly on TiO_2 particles. Thus the heterogeneous contribution seems to be involved in the observed differences as follows: no treatment $\leq$ P-FO $\approx$ V-UV < RF-P $\ll$ Ti-PC. The possible heterogeneous reactions involved in the degradation and mineralization of HQ are photo-Fenton oxidation (Eqs. (1)–(4) where =Fe(II) and =Fe(III) represent the surface Fe(II)/Fe(III) species) and semiconductor photocatalysis (Eqs. (5)–(9) where SC represent FeOOH or/and TiO_2 in the case of Ti-PC)

$$=Fe(II) + H_2O_2 \rightarrow =Fe(III) + OH^{\bullet} + OH^{-} \quad (1)$$

$$=Fe(III) + H_2O_2 \rightarrow =Fe(II) + HO_2^{\bullet} + H^{+} \quad (2)$$

$$=Fe(III)(OH)^{2+} + h\nu \rightarrow =Fe(II) + OH^{\bullet} \quad (3)$$

$$=Fe(III)L_n + h\nu \rightarrow =Fe(II)L_{n-1} + L_{ox}^{\bullet +} \quad (4)$$

$$SC + h\nu \rightarrow SC(e^{-} + h^{+}) \quad (5)$$

$$SC(e^{-}) + H_2O_2 \rightarrow SC + OH^{\bullet} + OH^{-} \quad (6)$$

$$SC(e^{-}) + =Fe(III) \rightarrow SC + =Fe(II) \quad (7)$$

$$SC(h^{+}) + R_{ad} \rightarrow SC + R_{ad}^{\bullet +} \quad (8)$$

$$SC(h^{+}) + H_2O \rightarrow SC + OH^{\bullet} + H^{+} \quad (9)$$

Fig. 5 shows the UV–vis absorption spectrum of several photocatalysts between 360 and 700 nm before their first use. The absorbance of PVF film in this region was negligible. The spectrum of PVF^{NT}-Fe oxide, $PVF^{V\text{-}UV}$-Fe oxide and $PVF^{P\text{-}FO}$-Fe oxide were similar and are thus represented by trace a. In contrast, $PVF^{RF\text{-}P}$-Fe oxide (trace b), and more markedly $PVF^{Ti\text{-}PC}$-Fe oxide (trace c) spectra show that the absorption was higher. The iron oxide on the polymer surface is responsible for the absorption of light. Hence the absorbance can be correlated with the thickness of iron oxide coating. These results show that RF-P and Ti-PC treatments favour iron oxide nucleation and/or deposition on the functionalized film and R_{ad} represents adsorbed organic species. On the contrary, P-FO and V-UV treatments did not improve significantly iron oxide deposition compared to no treatment.

Several causes could explain the beneficial effects induced by the functionalization of PVF surface: (i) a chemical functionalization where oxygen surface functionalities increase the surface polarity; (ii) the modification of polymer surface morphology induced by

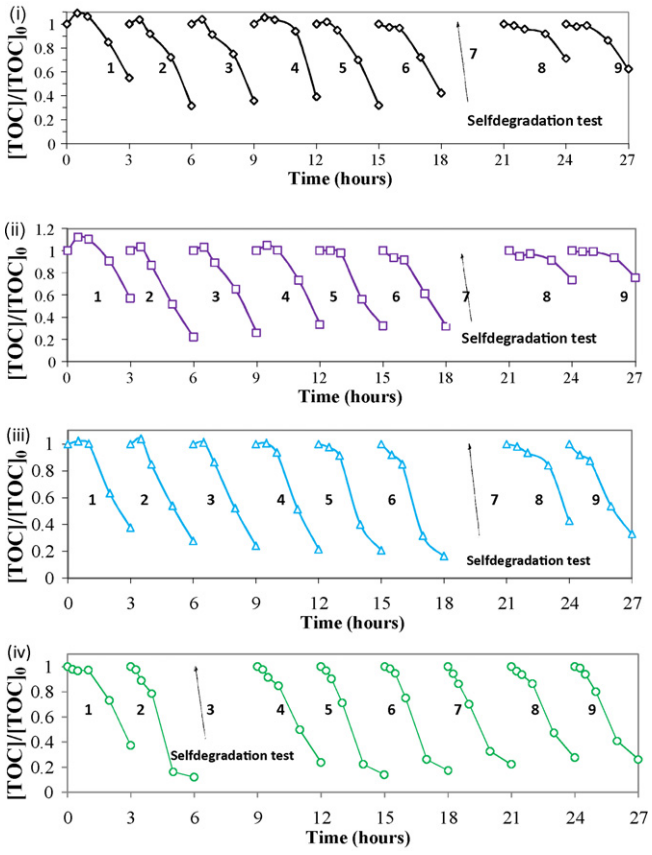

Fig. 6. TOC removal during repetitive HQ photocatalytic degradations by (i) PVF^{NF}-Fe oxide, (ii) $PVF^{V\text{-}UV}$-Fe oxide, (iii) $PVF^{RF\text{-}P}$-Fe oxide and (iv) $PVF^{Ti\text{-}PC}$-Fe oxide (experimental conditions: 0.18 mM of HQ, solar simulation, initial pH 5.7, H_2O_2 1.6 mM).

RF-P (etching) and by Ti-PC (deposition of particles); and (iii) the additional photocatalytic activity induced by the deposition of TiO_2 particles and likely synergistic effects with heterogeneous photo-Fenton oxidation [21]. The fact that V-UV and P-FO pre-treatments did not increase the photocatalytic activity of as prepared material (and by extension iron oxide deposition) can be explain by: (i) short V-UV treatment does not allow the production of polar groups like COOH on polymer surface and thus will not enhance iron oxide deposition; (ii) P-FO treatment may produce polar groups susceptible to bind iron oxide particles, however, iron aquacomplexes might immediately bind with this freshly formed polar moieties during the pre-treatment process.

3.3. Effect of functionalization on long-term stability of PVF^f-Fe oxide

The long term stability of several photocatalysts was tested repeating photo-Fenton HQ degradations experiments and applying a self-degradation test (SDT) that involved irradiation of the photocatalysts in absence of dissolved organic substance but in presence of H_2O_2. SDT simulates highly reactive conditions and aims to assess if the polymer substrate as well as overall photocatalytic activity are altered by radicals produced in absence of any organic compounds.

Fig. 6 shows repetitive HQ mineralization (eight cycles and one self degradation test). Between two runs, the catalyst and reactor system were thoroughly washed with distilled water. In Fig. 6(i) and (ii) (corresponding to PVF-Fe oxide and $PVF^{V\text{-}UV}$-Fe oxide, respectively) the photocatalytic activity remained constant during five cycles with about 60 and 70% TOC removal after 3 h of treatment. The SDT (after 18 h) induced an important and irreversible loss of 50% of photocatalytic activity (runs 8–9). For the $PVF^{RF\text{-}P}$-Fe oxide presented in Fig. 6(iii), irreversible catalytic activity loss of about 25% was observed after the SDT. In contrast, Fig. 6(iv) shows that for the $PVF^{Ti\text{-}PC}$-Fe oxide, the catalytic activity was recovered after the SDT (runs 4–5) and then decrease slowly. This recovery can be due to the presence of a thicker iron oxide shell (Fig. 5) and/or to a more solid binding of iron oxide particles to the polymer surface in the case of $PVF^{Ti\text{-}PC}$-Fe oxide than for the other catalysts.

These results show that the V-UV and PF-O functionalizations were not beneficial in term of final photocatalyst activity and long-term stability. In contrast, RF-P and Ti-PC functionalized materials shows higher stability and catalytic activity than not functionalized ones. Thus the formation of polar oxygen functionality on polymer surface as well as the increase of roughness allows the solid binding of iron oxide particles leading to stable photocatalysts. Besides for Ti-PC functionalization the presence of significant amount of TiO_2 particles on polymer surface can stabilize the photocatalyst acting as charge trap.

Because the TiO_2-PC functionalization led to the photocatalyst with the highest HQ degradation rates and long-term stability, this method was chosen for the comparison between PVF, PE and PET substrates and for the tests on bacterial inactivation.

3.4. Effect of polymer film nature on photocatalytic activity of $P^{Ti\text{-}PC}$-Fe oxide

Fig. 7 shows (i) TOC, (ii) HQ and (iii) $[Fe]_d$ over time during the HQ degradations experiments mediated by photocatalysts composed of three types of polymeric substrates (PVF, PE, PET) prepared under conditions slightly different than previously (i.e. TiO_2 1 g/L in the Ti-PC treatment and $FeCl_3$ 2 g/L in the hydrolysis step).

The photolysis test, in presence of H_2O_2 shows a slight increase of TOC (Fig. 7(i)) likely as a result of degradation and dissolution of both internal polymeric support and silicon rubbers used for water recirculation. Fig. 7(ii) shows that HQ was slowly degraded in presence of UV–vis radiation and H_2O_2, with about 25% decrease after 60 min of treatment. Besides, no significant HQ degradation was observed in presence of light only. During the photocatalytic experiment mediated by the supported iron oxide on Ti-PC functionalized PE, PET and PVF, HQ and TOC evolution were similar, reaching HQ total degradation between 60 and 90 min, and around 80% TOC decrease in 120 min. This fact indicates the low effect of the nature of polymer substrate on catalyst efficiency.

In contrast, Fig. 7(iii) shows that the amount of leached iron ions was dependant on the polymer nature with a maximum around 1.1, 0.9 and 0.7 mg/L after 120 min of treatment for PET, PVF and PE, respectively. The amounts of dissolved iron observed in this experiment for the PVF substrate were higher than those displayed in Fig. 1(iii), probably due to the difference in the catalyst preparation procedure. However three of the catalysts polymeric substrates used in the experiments of Fig. 7, were prepared with the same procedure and, thus, comparison is possible. A larger iron leaching could be linked to larger iron oxides quantities adsorbed on the substrate and, by extension, to the achievement of more surface functionalization in the pre-treatment, and to the own nature of substrate (higher polarised surface).

3.5. Elucidation of the role played by homogeneous photo-Fenton chemistry.

Since homogeneous photo-Fenton reactions seem to play an important role in the above described degradation of HQ and TOC removal due to the presence of significant quantities of dissolved iron species, a set of experiments were carried out in order to distinguish between the contributions of homogeneous photo-Fenton,

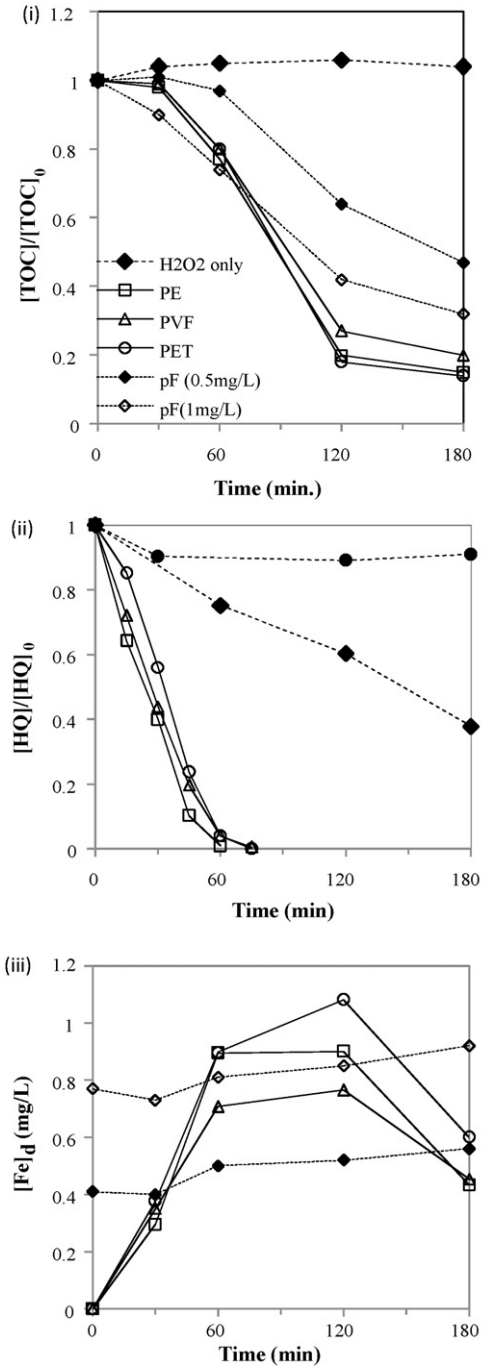

Fig. 7. Evolution of (i) TOC, (ii) HQ concentration and (iii) $[Fe]_d$ during degradation of 0.18 mM of HQ at initial pH 5.7, in presence of 1.6 mM H_2O_2, 75 cm^2 of catalyst ($PE^{Ti\text{-}PC}$-Fe oxide, $PVF^{Ti\text{-}PC}$-Fe oxide, $PET^{Ti\text{-}PC}$-Fe oxide, Fe^{2+}) under solar simulation for different polymeric substrates. The traces represent an average over three runs.

heterogeneous photo-Fenton (Eqs. (1)–(4)), TiO_2 and iron oxide heterogeneous photocatalysis (Eqs. (4)–(9)).

Two experiments using typical conditions of the above polymer-based experiments with 0.5 and 1.0 mg/L of Fe^{3+} added to the initial solutions were carried out (Fig. 7(i)). The amounts of Fe^{3+} were selected taking into account that for polymers tested section 3.3: (a) the amount of free Fe^{3+} in solution after 60 min (and at the end of the treatment) was around 0.4 mg/L; (b) this amount increased to a maximum of 0.7–0.9 mg/L after 120 min (Fig. 7(iii)). These experiments simulate the homogeneous contribution due to dissolved iron ions in the heterogeneous system. Nevertheless these

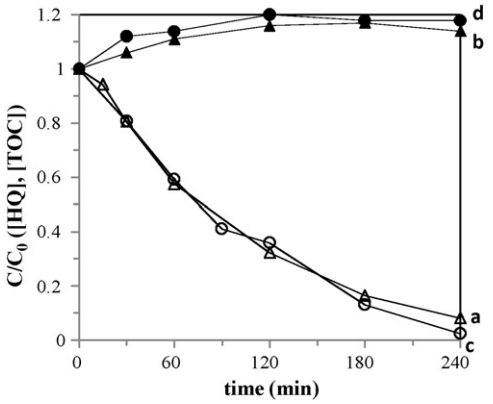

Fig. 8. Evolution of HQ concentration and TOC during degradation of HQ mediated by $PVF^{Ti\text{-}PC}$ ((a) and (b), respectively) and $PVF^{Ti\text{-}PC}$-Fe oxide ((c) and (d), respectively) (experimental conditions: 0.18 mM of HQ, solar simulation, controlled pH 6, H_2O_2 1.6 mM).

results are only indicative since in the case of heterogeneous system, the dissolved iron concentration is time-dependant and the optical properties of the reactor changes due to the presence of polymer film photocatalyst.

Larger mineralizations were always observed with the heterogeneous systems, making clear that the observed chemistry is not only of homogeneous character and pointing toward a remarkable contribution of the heterogeneous reactions (Fig. 7(i)) were a 20% increase of the mineralization rate is noticed in presence of the polymer film photocatalyst if compared to homogeneous photo-Fenton (1 mg/L).

In order to avoid the occurrence of homogeneous photo-Fenton reactions, additional experiments under controlled pH conditions were carried out. The solution pH was kept constant around 6 by periodical additions of a concentrated H_2SO_4 solution. In this way, release of free Fe^{2+} and Fe^{3+} to the solution was minimized. The changes observed in HQ concentration and TOC values then could be assigned to heterogeneous chemistry. As can be seen in Fig. 8, during 180 min of reaction, the HQ concentration follows almost the same time-course either using the $PVF^{Ti\text{-}PC}$-Fe oxide or the $PVF^{Ti\text{-}PC}$ catalysts. Concerning TOC removal both catalysts show a poor activity as can be seen in Fig. 8. Even a slight increase of TOC along reaction time is noticed. This could only be explained by considering partial degradation of the organic support and organic release to the solution.

Apart from differences between the two catalysts such as different quantities of TiO_2 and the presence or not of large amounts of iron oxide at photocatalyst surface (Table 1), the former result could indicate that at controlled pH 6, supported TiO_2 photocatalysis is the main contributor to the heterogeneous chemistry. Iron oxide contribution via SC photocatalysis (Eqs. (5)–(9)) and/or heterogeneous photo-Fenton (Eqs. (1)–(4)) which was significant at acidic pHs (4.5 section 3.2) appears to be low under these conditions.

In this sense, the improvement of the polymer-catalyst couple should be the object of further research. Either the synthesis of TiO_2-iron oxide mixtures strongly attached to the polymers, or the increase of the catalyst films thickness, or changes of the TiO_2-iron oxide proportion or composition would possibly minimize the effect of solution pH changes or the consequences of the photocatalysis toward the polymeric support itself.

3.6. Bacterial inactivation

The ability of $PET^{Ti\text{-}PC}$-Fe oxide to inactivate the indicator bacteria *E. coli* in presence of H_2O_2 and light was investigated in batch reactor. However this material was found to constitute a light filter

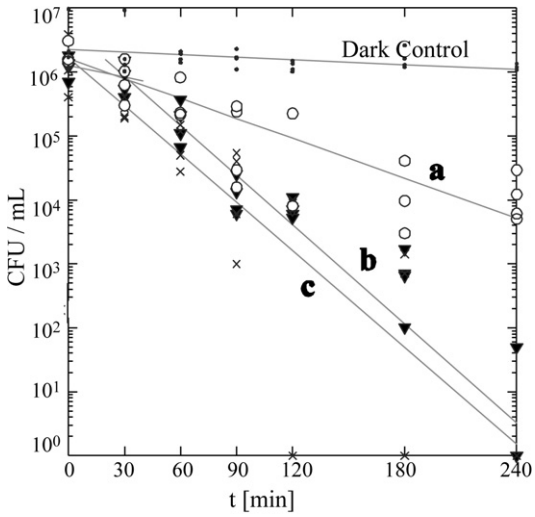

Fig. 9. Inactivation of *E. coli* on PET bottle reactors (experimental conditions presented in Table 2).

to the incoming light, protecting bacteria suspension from direct radiation. The protective effect was not observed in the case of HQ degradation because the reactor setup was different (the internal opaque PVC support make the photochemical reaction possible only between internal surface of Pyrex reactor and the surface of photocatalyst films) and because in contrast with *E. coli*, HQ is resistant to photolysis (Fig. 9).

Then PET bottles (PET_b) were used as catalyst support and their bottom were functionalized and coated with iron oxide (to let the light pass through the suspension) leading to $PET_b^{Ti\text{-}PC}$-Fe oxide. The inactivation of *E. coli* suspended in pure water under simulated solar light was measured in PET_b reactor in presence of Fe^{3+} and H_2O_2. Simultaneously, inactivation mediated by $PET_b^{Ti\text{-}PC}$-Fe oxide in presence of H_2O_2 and the photolytic inactivation were measured. Fig. 9 shows first order exponential fittings (lines) calculated in Matlab ($N_t = N_0 e^{k_{obs} \times t}$). Table 2 shows the composition of the suspension matrices, the experimental conditions for the different systems and observed inactivation rates (k_{obs} (min^{-1})). Fig. 9 shows that the heterogeneous system ($PET_b^{Ti\text{-}PC}$-Fe oxide/H_2O_2/light) has a higher bactericidal effect as the homogenous system (Fe^{3+}/H_2O_2/light) in PET bottles (both $k_{obs} \approx 0.6\,min^{-1}$). Similar experiments using H_2O_2 (0.3 mM) and light, have shown that bacterial inactivation rates were similar to those when using light only (results not shown here [5]). Besides as the rates of compounds degradation by P^{TiPC}-Fe oxide/light were an order of magnitude lower than when using P^{TiPC}-Fe oxide/light/H_2O_2 [21], the heterogeneous system is supposed to be inefficient as well for bacterial inactivation in the absence of hydrogen peroxide.

Iron ions concentrations in the filtered samples was below the detection limit (<0.1 mg/L) for both heterogeneous and homogeneous systems. Different explanations can justify the absence of detectable dissolved iron when using PET bottles: (i) the inactivation may takes place on bottle surface (on iron or titanium oxide for heterogeneous system, and iron complexes adsorbed on bottle surface for homogeneous system), and (ii) the dissolved iron species may also be adsorbed on bacteria surface or even enter the intracellular medium and this contact could significantly contribute to the effective photo-inactivation [5].

Table 2
Experimental conditions and observed rate constants for the bacterial inactivation tests in PET bottle reactors under simulated solar radiation.

	Photocatalyst	H_2O_2 (mM)	k_{obs} (min^{-1})
a	–	–	0.024 ± 0.004
b	Fe^{3+} (0.6 mg/L)	0.3	0.053 ± 0.008
c	$PET_b^{Ti\text{-}PC}$-Fe-oxide	0.3	0.060 ± 0.004

4. Conclusions

Implement a functionalization of polymer surface can be an efficient strategy to improve the attraction between iron oxide and polymer film supports, leading to more efficient photocatalysts. Besides functionalization process such as Ti-PC can concomitantly lead to the deposition of additional active specie (TiO_2 particles).

- Among the different functionalization processes studied here, RF-P and more markedly Ti-PC treatments were useful to improve photocatalytic activity and long-term stability.
- PVF, PE or PET supports led to catalysts showing similar photoactivity ruling out the possibility that the polymer nature influence significantly the catalyst efficiency.
- However significant amounts of dissolved iron species leached from catalyst substrate lead to important homogeneous photo-Fenton contribution.
- $PVF^{Ti\text{-}PC}$-Fe oxide was not an efficient material to mineralize HQ at controlled neutral pH. Under these conditions, HQ degradation was slow and mostly caused by TiO_2 photocatalysis and the heterogeneous photo-Fenton process contributed only in a minor way.

PET bottle employed as reactors and catalysts support ($PET_b^{Ti\text{-}PC}$-Fe oxide) was an efficient heterogeneous photocatalyst to inactivate bacteria and no dissolved iron ions were detected in the filtered solution opening perspectives for SODIS applications.

Acknowledgments

F. Mazille wishes to express his gratitude to Robin Humphry-Baker, Nicolas Xanthopoulos and Pierre-Yves Pfirter for surface analysis and to John Kiwi for reviewing of phrasing. The authors wish to thank the European Commission for funding the INNOWATECH Project (Contract No. 036882) under the thematic priority Global Change and Ecosystems of the Sixth Framework Program (FP6-2005-Global 4—SUSTDEV-2005-3.II.3.2).

References

[1] S. Malato, P. Fernández-Ibáñez, M.I. Maldonado, J. Blanco, W. Gernjak, Decontamination and disinfection of water by solar photocatalysis: Recent overview and trends, Catal. Today 147 (2009) 1–59.
[2] A.G. Rincon, C. Pulgarin, Absence of *E. coli* regrowth after Fe^{3+} and TiO_2 solar photoassisted disinfection of water in CPC solar photoreactor, Catal. Today 124 (2007) 204–214.
[3] A. Moncayo-Lasso, J. Sanabria, C. Pulgarin, N. Benítez, Simultaneous *E. coli* inactivation and NOM degradation in river water via photo-Fenton process at natural pH in solar CPC reactor. A new way for enhancing solar disinfection of natural water, Chemosphere 77 (2009) 296–300.
[4] F. Sciacca, J.A. Rengifo-Herrera, C. Pulgarin, Dramatic enhancement of solar disinfection (SODIS) of wild *Salmonella* sp. in PET bottles by H2O2 addition on natural water of Burkina Faso containing dissolved iron, Chemosphere 78 (2010) 1186–1191.
[5] D. Spuhler, J.A. Rengifo-Herrera, C. Pulgarin, The effect of Fe^{2+}, Fe^{3+}, H_2O_2 and the photo-Fenton reagent at near neutral pH on the Solar Disinfection (SODIS) at low temperatures of Water containing *E. coli* K12, Appl. Catal. B (2010), doi:10.1016/j.apcatb.2010.02.010.
[6] N.F. Gray, Drinking Water Quality Problems and Solutions, second ed., Cambridge University Press, 2008, p. 335.
[7] J. He, X. Tao, W. Ma, J. Zhao, Heterogeneous photo-Fenton degradation of an azo dye in aqueous H_2O_2/iron oxide dispersions at neutral pHs, Chem. Lett. 1 (2002) 86–87.
[8] A. Bozzi, T. Yuranova, J. Mielczarski, J. Kiwi, Evidence for immobilized photo-Fenton degradation of organic compounds on structured silica surfaces involving Fe recycling, New J. Chem. 28 (2004) 519–526.
[9] M. Noorjahan, V. Durga Kumari, M. Subrahmanyam, L. Panda, Immobilized Fe(III)-H.Y: an efficient and stable photo-Fenton catalyst, Appl. Catal. B 57 (2005) 291–298.

[10] J. Feng, X. Hu, P.L. Yue, Effect of initial solution pH on the degradation of Orange II using clay-based Fe nanocomposites as heterogeneous photo-Fenton catalyst, Water Res. 40 (2006) 641–646.
[11] I. Muthuvel, M. Swaminathan, Photoassisted Fenton mineralisation of Acid Violet 7 by heterogeneous Fe(III)-Al_2O_3 catalyst, Catal. Commun. 8 (2007) 981–986.
[12] A. Moncayo-Lasso, R.A. Torres-Palma, J. Kiwi, N. Benítez, C. Pulgarin, Bacterial inactivation and organic oxidation via immobilized photo-Fenton reagent on structured silica surfaces, Appl. Catal. B 84 (2008) 577–583.
[13] T. Liu, H. You, Q. Chen, Heterogeneous photo-Fenton degradation of polyacrylamide in aqueous solution over Fe(III)-SiO_2 catalyst, J. Hazard. Mater. 162 (2009) 860–865.
[14] O. Akhavan, R. Azimirad, Photocatalytic property of Fe_2O_3 nanograin chains coated by TiO_2 nanolayer in visible light irradiation, Appl. Catal. A 369 (2009) 77–82.
[15] B. Sommer, A. Mariño, Y. Solarte, M.L. Salas, C. Dierolf, C. Valiente, D. Mora, R. Rechsteiner, P. Setter, W. Wirojanagud, H. Ajarmeh, A. Al-Hassan, M. Wegelin, SODIS—an emerging water treatment process, J. Water SRT—Aqua 46 (1997) 127–137.
[16] M. Kosmulski, E. Maczka, E. Jartych, J.B. Rosenholm, Synthesis and characterization of goethite and goethite–hematite composite: experimental study and literature survey, Adv. Colloid Interface Sci. 103 (2003) 57–76.
[17] C.-M. Chan, T.-M. Ko, H. Hiraoka, Polymer surface modification by plasmas and photons, Surf. Sci. Rep. 24 (1996) 1–54.
[18] T. Yuranova, A.G. Rincon, A. Bozzi, S. Parra, C. Pulgarin, P. Albers, J. Kiwi, Antibacterial textiles prepared by RF-plasma and vacuum-UV mediated deposition of silver, J. Photochem. Photobiol. A 161 (2003) 27–34.
[19] M.I. Mejia, J.M. Marin, G. Restrepo, C. Pulgarin, E. Mielczarski, J. Mielczarski, Y. Arroyo, J.-C. Lavanchy, J. Kiwi, Self-cleaning modified TiO_2-cotton pretreated by UVC-light (185 nm) and RF-plasma in vacuum and also under atmospheric pressure, Appl. Catal. B 91 (2009) 481–488.
[20] G.G. Kim, J.A. Kang, J.H. Kim, S.J. Kim, N.H. Lee, S.J. Kim, Metallization of polymer through a novel surface modification applying a photocatalytic reaction, Surf. Coat. Technol. 201 (2006) 3761–3766.
[21] F. Mazille, T. Schoettl, C. Pulgarin, Synergistic effect of TiO_2 and iron oxide supported on fluorocarbon films. Part 1: Effect of preparation parameters on photocatalytic degradation of organic pollutant at neutral pH, Appl. Catal. B 89 (2009) 635–644.
[22] M.M. Gibbs, A simple method for the rapid determination of iron in natural waters, Water Res. 13 (1979) 295–297.
[23] F. Mazille, A. Lopez, C. Pulgarin, Synergistic effect of TiO_2 and iron oxide supported on fluorocarbon films. Part 2. Long-term stability and influence of reaction parameters on photoactivated degradation of pollutants, Appl. Catal. B 90 (2009) 321–329.
[24] M.A. Golub, T. Wydeven, R.D. Cormia, ESCA study of several fluorocarbon polymers exposed to atomic oxygen in low Earth orbit or within or downstream from a radio-frequency oxygen plasma, Polymer 30 (1989) 1571–1575.
[25] M.L. Everett, G.B. Hoflund, Chemical alteration of poly(vinyl fluoride) Tedlar® induced by exposure to vacuum ultraviolet radiation, Appl. Surf. Sci. 252 (2006) 3789–3798.
[26] T. Yamashita, P. Hayes, Analysis of XPS spectra of Fe^{2+} and Fe^{3+} ions in oxide materials, Appl. Surf. Sci. 254 (2008) 2441–2449.
[27] E.A. Deliyanni, L. Nalbandian, K.A. Matis, Adsorptive removal of arsenites by a nanocrystalline hybrid surfactant-akaganeite sorbent, J. Colloid Interface Sci. 302 (2006) 458–466.
[28] S. Musicĭ, S. Krehula, S. Popovicĭ, Ž. Skoko, Some factors influencing forced hydrolysis of $FeCl_3$ solutions, Mater. Lett. 57 (2003) 1096–1102.